ELSEVIER

Marine Geology 177 (2001) 25–44

MARINE GEOLOGY
INTERNATIONAL JOURNAL OF MARINE GEOLOGY, GEOCHEMISTRY AND GEOPHYSICS

www.elsevier.nl/locate/margeo

High-resolution geochemical and micropalaeontological profiling of the most recent eastern Mediterranean sapropel

D. Mercone, J. Thomson*, R.H. Abu-Zied, I.W. Croudace, E.J. Rohling

Southampton Oceanography Centre, Empress Dock, Southampton SO14 3ZH, UK

Received 1 June 1999; accepted 29 December 2000

Abstract

A combined geochemical and micropalaeontological study of the most recently-deposited sapropel (S1) from the eastern Mediterranean Sea is reported from two cores in which the S1 sapropel units were rapidly deposited (15 and 20 cm ky^{-1}). Such rapid accumulation rates have largely protected the two S1 units from post-depositional oxidation effects and allow a high-resolution investigation of conditions before, during and after S1 formation. The cores are from the Adriatic and Aegean Seas, and both record a simultaneous diminution in intensity of sapropel development at 7500 conventional radiocarbon years that divides both visual S1 units into two approximately equal lobes. Detailed foraminiferal analysis of the Aegean core reveals fluctuations in benthic foraminifera species that indicate anoxic or near-anoxic bottom water conditions during formation of the upper and lower lobes. The central S1 section shows a temporary repopulation by an opportunistic benthic species (*G. orbicularis*) indicative of improved bottom water oxygen levels. The appearance and disappearance of this species in the central section, and its reappearance just before the end of S1 times, also coincides with increases in abundance of pelagic foraminifera characteristic of cooler surface water conditions, and with local Mn peaks in the sapropel. These features are interpreted as indications of increased deep-water ventilation and bottom water O_2 levels centred during S1 time. Although the S1 C_{org} contents are low at 1–2 wt.% because of dilution by high detrital fluxes, a set of elements (Ba, Cr, Cu, Mo, Ni, S, Se, U, V and Zn) generally present in other S1 units, older sapropels and black shales is clearly present at enhanced levels. Sulfur enrichment is well correlated with the C_{org} content throughout S1, and FeS_2 formation accounts for the bulk of the observed S enrichment.

Keywords: Mediterranean Sea; Sapropel; Barium; Trace elements; Redox

1. Introduction

Whereas the sediments laid down in the eastern Mediterranean Sea are normally C_{org} poor, C_{org}-rich units termed sapropels also form episodically over most of the basin (Ryan, 1972; Cita et al., 1977; Vergnaud-Grazzini et al., 1977; Emeis et al., 1996). There is a cyclicity in the timing of sapropel deposition that correlates with variations in the earth's orbital eccentricity and axial precession and obliquity (Rossignol-Strick et al., 1982; Hilgen, 1991; Lourens et al., 1996; Langereis et al., 1997). The critical local expression of these orbital variations for sapropel formation appears to be the establishment of strong seasonal monsoon conditions in the North African region (Rossignol-Strick, 1983, 1985; Rohling and Hilgen, 1991). While it seems well established that sapropels always form at these times of enhanced

* Corresponding author. Tel.: +23-8059-6548; fax: +23-8059-6554.

E-mail address: john.thomson@soc.soton.ac.uk (J. Thomson).

0025-3227/01/$ - see front matter
PII: S0025-3227(01)00122-0

rainfall and river run-off, however, the mechanism by which the basin water column responds to the resultant climatic change so as to cause sapropel deposition is less certain (Rohling, 1994; Myers et al., 1998; Bethoux and Pierre, 1999). Higher C_{org} productivity or improved C_{org} preservation must be involved, and there is good evidence for both (Cita and Grignani, 1982; Calvert, 1983; Rohling and Gieskes, 1989; Fontugne and Calvert, 1992; Castradori, 1993; Jorissen, 1999). It is likely that integrated investigations involving the micropalaeontology, geochemistry and sedimentology of sapropels and their surrounding sediments will be required to elucidate mechanisms of change in the basin's water column, and the transitions into and out of the sapropel deposition mode.

Although the most recent Holocene sapropel (S1; Hieke, 1976) never develops the high C_{org} contents seen in some older sapropels, its recent deposition (9–6 ka BP) and its amenability to precise radiocarbon dating make it a favoured research target. Detailed geochemical studies of S1 have revealed that many S1 units have already suffered a post-depositional oxidative alteration that has resulted in extensive diagenetic relocation of several elements (Ten Haven et al., 1987; de Lange et al., 1989; Higgs et al., 1994; Thomson et al., 1995; van Santvoort et al., 1996). This work attempts to circumvent such post-depositional geochemical alterations by investigating rapidly-accumulated S1 units. The premise is that rapid accumulation will remove the sapropel sediments from diffusional contact with bottom water oxygen shortly after formation, so that there is a greater probability of finding the original elemental associations in the S1 units.

A second aspect of high deposition-rate S1 units is that some of these have revealed a structure within S1 that is not recognized in most E. Mediterranean cores where S1 units are single dark intervals with clearly-defined tops and bases. In rapidly-accumulated cores, mostly but not exclusively from the Adriatic and Aegean Seas, a lighter-coloured central section often divides the dark interval into two roughly-equal halves (Rohling et al., 1997). At present it is not certain whether lighter S1 central sections are preferentially evident as a consequence of the improved resolution provided by rapid deposition, or whether they are restricted to particular areas of the eastern Mediterranean basin. The selected cores are from the Adriatic and Aegean Seas, both display double S1 units, and both have already been dated by the radiocarbon method. They therefore provide the opportunity to compare and contrast the geochemical and micropalaeontogical changes in sediment deposited through S1 times.

2. Material and methods

Giant piston cores MD90–917 (41° 18′N, 17° 37′E, 1010 m water depth from the Adriatic Sea) and LC21 (35° 40′N, 26° 35′E, 1522 m water depth from the SE Aegean Sea) were sampled at the core archives at the Laboratoire des Sciences du Climat et de L'Environnement, Gif-sur-Yvette and the British Ocean Sediment Core Repository (BOSCOR), Southampton, respectively. In LC21, the dark units identified as contemporaneous with S1 were at 138–162 cm (upper lobe), 162–172 cm (lighter central section) and 172–195 cm (lower lobe), and in core 90–917 at 223–239 cm (upper lobe), 239–245 cm (central section) and 245–256 cm (lower lobe).

The cores were sub-sampled at 1 cm resolution above, through, and below the S1 units. For geochemistry, sufficient sediment was taken to give a dry weight of >3 g, and samples were freeze-dried then ground and homogenized using a tungsten carbide swing mill. Major and minor elements were determined using a Philips PW1400 automatic sequential wavelength dispersive X-ray fluorescence spectrometer on samples prepared either as pressed powder pellets or as lithium meta-tetraborate fusion discs. Accuracy and precision were ascertained by running the international standard reference material MAG-1 (marine mud); the precision for trace element determination was 5% relative standard deviation (r.s.d), whilst for major element analyses it was typically $<1\%$ r.s.d. Organic carbon (C_{org}) and $CaCO_3$ were determined coulometrically via the release of CO_2. Calcium carbonate was determined by the generation of CO_2 evolved by the addition of 10% (v/v) H_3PO_4, and C_{org} by subtraction of the CO_2 evolved from $CaCO_3$ from the CO_2 derived from total sample combustion at 900°C. Precision for both $CaCO_3$ and C_{org} analyses were determined by replicate analysis of an in-house standard (a deep-sea carbonate sediment)

at <1% r.s.d. for $CaCO_3$ and <3% r.s.d for C_{org} measurements, respectively.

Samples for foraminiferal study were typically >1 g dry weight. Samples were dried at 50°C for at least 24 h, weighed, and soaked in demineralized water. Once disaggregated, samples were passed through 63, 125, 150 and 600 μm sieves, rinsed with demineralized water, and the sieved fractions dried and weighed. The 150–600 μm fraction was split into suitable aliquots containing at least 200 planktonic foraminifera, which were speciated and stored in multi-cell faunal slides. Benthic foraminifera were extracted from the entire 150–600 μm fraction for all samples, and similarly sorted and stored.

3. Results and discussion

3.1. Radiocarbon, benthic and planktonic foraminifera evidence

The overall accumulation rates of the dark-coloured layers and lighter-coloured central sections in cores MD90–917 and LC21 have been estimated at 20 and 15 cm ky^{-1}, respectively, by AMS radiocarbon dating of >150 μm planktonic foraminifera fractions (Mercone et al., 2000). These rates contrast with S1 units deposited in deeper water, where accumulation rates are as low as 3 cm ky^{-1}. The same radiocarbon data have established that these dark units are contemporaneous with S1, and that the central sections are near-contemporaneous and centred on 7500 radiocarbon convention years. The apparent durations of the central sections differ slightly, however, at 700 years in core LC21 compared with 250 years in core MD90–917. Neither central section appears to be the result of any sediment redistribution process because the radiocarbon ages increase regularly and monotonically with depth through both units (Mercone et al., 2000).

The planktonic foraminiferal data for core LC21 (De Rijk et al., 1999) indicate that while the species grouping indicative of warm surface waters (*G. ruber*, *G. rubescens*, *G. tenella*, *G. siphonifera*, *G. sacculifer*, *O. universa* and *G. digitata*) was generally exclusive during the formation of both the upper and lower S1 lobes, the central section corresponds to a short period when colder water species (*T. quinqueloba*, *G. scitula*, *N. pachyderma* and *G. inflata*) appear suddenly in the record and then disappear more gradually (Fig. 1). Another gradual surface-water cooling trend occurs towards the end of the upper S1 lobe, but warm-water species do not again become exclusive until well after the end of S1. The most likely mechanism for short-term cooling events in the Aegean Sea is through intensified winter outbreaks of orographically-channeled, cold, dry, high-latitude air from the north (Mariolopoulos, 1961; Leaman and Schott, 1991; Poulos et al., 1997).

Only a few samples in the LC21 sapropel show a total absence of benthic foraminifera, but compared with the enclosing sediments the number of benthic specimens per gram and the number of species identified are both consistently at very low levels throughout the upper and lower S1 lobes and the central section (Fig. 1). Occasional epiphytic benthic foraminiferal specimens are found that likely originate from shallower well-oxygenated waters (through 'rafting' on phytodetritus), but the benthic foraminifera found within both sapropel lobes are predominantly of the species *Chilostomella mediterranensis*, *Rutherfordoides rotundiformis* and *Globobulimina affinis*. These species are tolerant to extremely low oxygen conditions (Rohling et al., 1997). Persistent anoxia at the sea floor would cause a total absence of benthic foraminifera, so that the presence of this group of 'Oxygen Deficiency Stress' (ODS) tolerant species either indicates intermittent anoxia or continuous severe dysoxia at the sea floor (Fig. 1). The opportunistic species *G. orbicularis*, which requires a finite bottom water O_2 concentration (Jorissen, 1999), colonises the central section, disappears in the lower part of upper S1 lobe, and then returns in the upper lobe at the same time as cool water planktonic species reappear. The coincidence of the appearances of *G. orbicularis* in the benthic record with the times of colder surface water indicated by the planktonic record is striking (Fig. 2). Given that the Aegean Sea is known to be an occasional but substantial source area for Mediterranean deep-water formation (Klein et al., 1999; Theocharis et al., 1999), this coincidence is likely to be caused by improved oxygenation as a consequence of episodes of new bottom water formation. The dominance of the ODS group during formation of most of the upper and lower organic–rich units means that bottom waters were

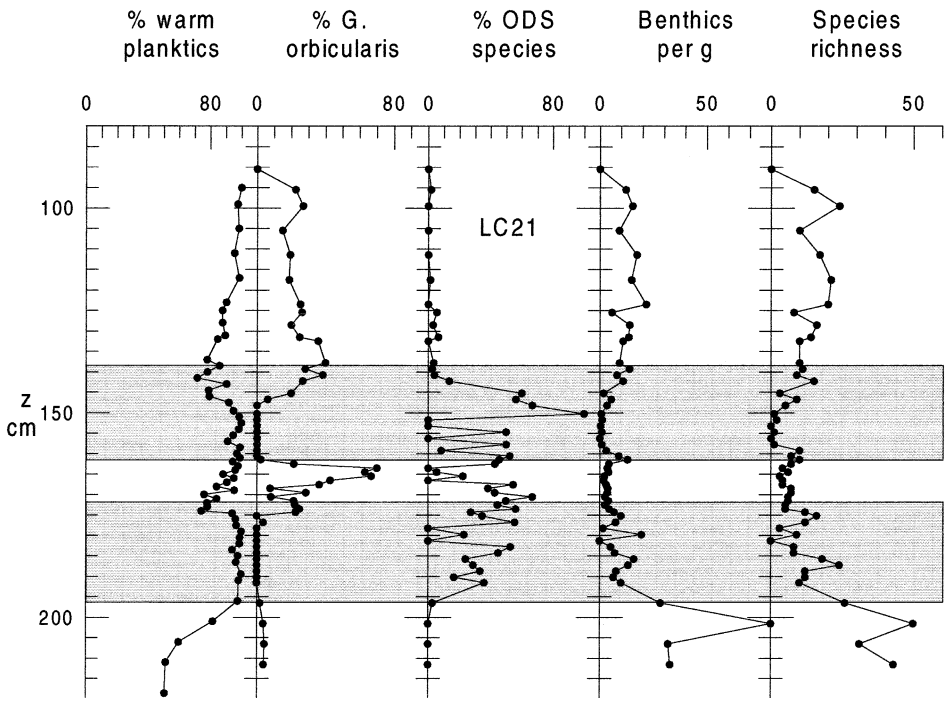

Fig. 1. Foraminiferal data for core LC21 (35° 40′N, 26° 35′E, 1522 m water depth, SE Aegean Sea) as functions of depth. From left: planktonic foraminifera expressed as percentage of warm (*G. ruber*, *G. rubescens*, *G. tenella*, *G. siphonifera*, *G. sacculifer*, *O. universa* and *G. digitata*) versus cold (*T. quinqueloba*, *G. scitula*, *N. pachyderma* and *G. inflata*) species (from De Rijk et al., 1999); *G. orbicularis* as % of all benthic specimens; 'oxygen deficit species' (ODS, *Chilostomella mediterranensis*, *Rutherfordoides rotundiformis* and *Globobulimina affinis*), as % of all benthic specimens; number of benthic specimens per gram and benthic foraminiferan species richness (i.e. number of species recognized). The two dark coloured lobes in S1 are shaded (upper: 138–162 cm, lower: 172–195 cm).

likely to have been anoxic-non-sulfidic rather than anoxic-sufidic at this location during S1 times, while the appearance of *G. orbicularis* indicates episodes of more oxic bottom water conditions.

No foraminifera data have been gathered for core MD90–917, but data from another nearby Adriatic core with a double S1 sapropel have been reported by Jorissen et al. (1993) and Rohling et al. (1997). In that core the lower S1 lobe was devoid of benthic fauna, but there was a temporary re-establishment of a benthic fauna in the lighter central section that showed a weak continuation into the upper S1 lobe. In that case the benthic repopulations in the central section and at the top of S1 again coincided with increased abundances of cool water planktonic species (Rohling et al., 1997; De Rijk et al., 1999). Since the Adriatic is the best-known source area of deep waters to the eastern Mediterranean (Malanotte-Rizzoli and Hecht, 1988), it seems likely that cooling events caused improved ventilation and consequently benthic repopulation in that area also.

3.2. Geochemical evidence: Ba and C_{org}

Sapropel sequences have been reported where repetitive changes in the relative magnitudes of eolian, fluviatile and productivity input fluxes result in a cyclicity in the major element composition of the sediments (Wehausen and Brumsack, 1999). These cyclicities are revealed as changes in the relative proportions of major elements with depth (e.g. $CaCO_3$ content, Si/Al, Ti/Al, Mg/Al, K/Al and Zr/Al ratios). These same element/Al ratios can also reveal the presence of ash layers or turbidites. In the two cores studied, only a short period around S1 times has been investigated, and changes in the Al-normalized ratio profiles are modest for these same elements (Figs. 2 and 3). Together with the regular progression

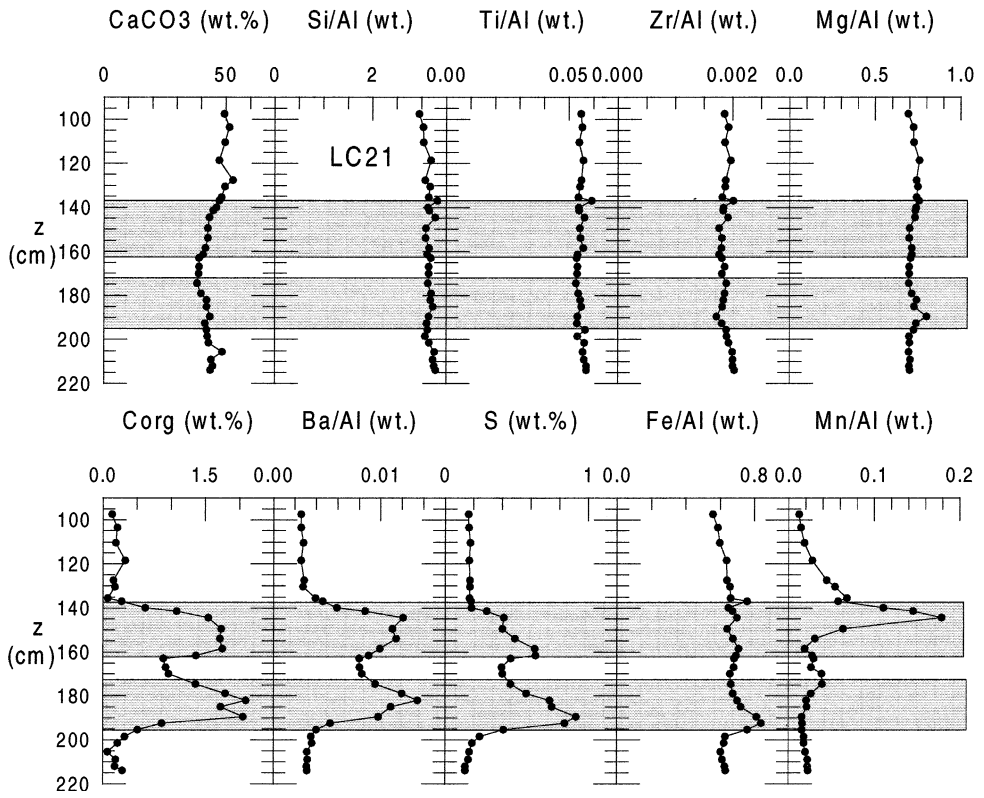

Fig. 2. Concentration ($CaCO_3$, C_{org} and S, wt.%) and Al-normalised concentration (Si, Ti, Zr, Mg, Ba, Fe and Mn) versus depth profiles for core LC21. The two dark coloured lobes in S1 are shaded (upper: 138–162 cm, lower: 172–195 cm).

of radiocarbon age with depth (Mercone et al., 2000), this approximately constant composition is taken as evidence that the sampled sections of the two cores are not affected by redeposition processes. Marked excursions observed in the profiles of other elements will be interpreted as caused by redox processes or C_{org}- or S-associations.

While rapid accumulation rates have protected the S1 units in these two cores from post-depositional oxidation, another consequence is that their C_{org} contents are diluted to low levels by the high detrital input flux. In fact only a few levels in core LC21 and none in core 90–917 achieve the $>2\%$ C_{org} level proposed by Kidd et al. (1978) to define a sapropel (Figs. 2 and 3). In accord with the visual evidence, the C_{org} concentration versus depth profiles through S1 in both cores are in the form of upper and lower lobes of higher values with a central saddle of lower values corresponding to the lighter section. In neither case, however, do the C_{org} values in the central sections fall as low as the values observed before and after S1.

Barium is an element that is progressively concentrated with organic material during settling between its production and deposition, as demonstrated by sediment trap studies (Dymond et al., 1992; Francois et al., 1995), although the mechanism of Ba uptake by the settling material remains to be identified (Dymond and Collier, 1996). The relative persistence of Ba compared with C_{org} has made it a favoured palaeoproductivity indicator for sapropels (Calvert, 1983; van Os et al., 1991; Thomson et al., 1995; van Santvoort et al., 1996; Langereis et al., 1997). The excess Ba in the S1 units investigated can be visualised through normalization to Al, recognizing that a substantial Ba contribution is present in detrital aluminosilicate phases (Figs. 2 and 3). This excess Ba of the S1 sediments compared with the enclosing sediments may be evaluated by subtracting an

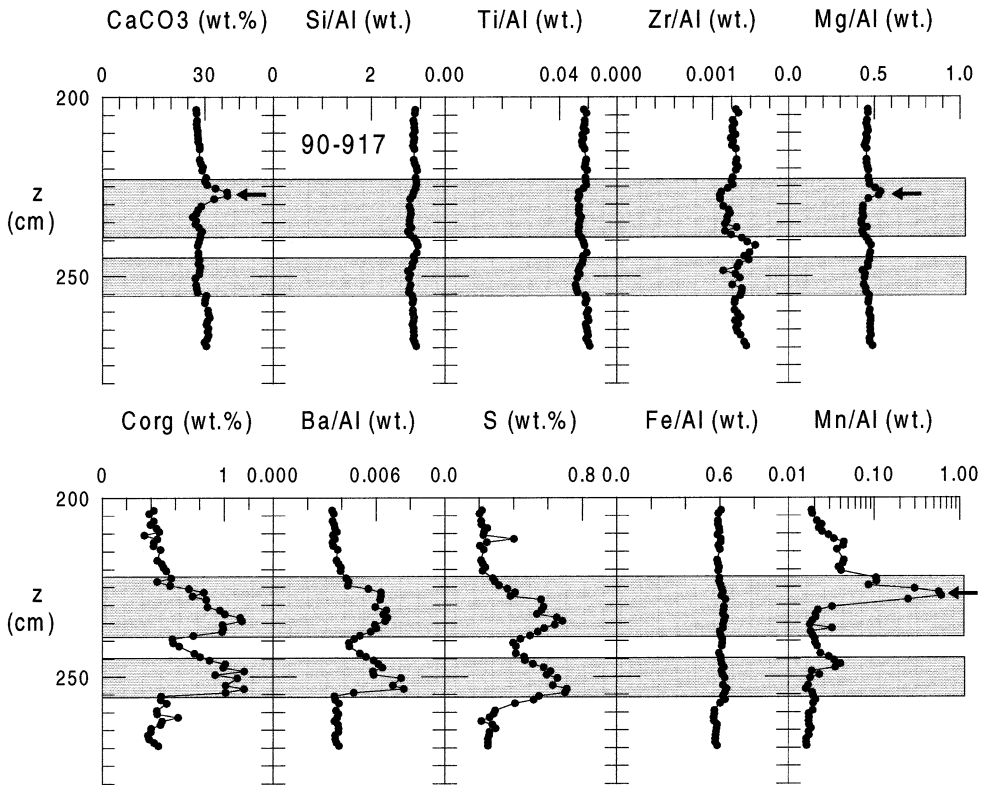

Fig. 3. Concentration ($CaCO_3$, C_{org} and S, wt.%) and Al-normalised concentration (Si, Ti, Zr, Mg, Ba, Fe and Mn) versus depth profiles for core MD90–917 (41° 18′N, 17° 37′E, 1010 m water depth, Adriatic Sea). The two dark coloured lobes in S1 are shaded (upper: 223–239 cm, lower: 245–256 cm). Three arrows indicate coincident local maxima in the $CaCO_3$, Mg/Al and Mn/Al profiles indicative of kutnahorite (see text).

anticipated detrital level for Ba estimated from the measured Al value:

$$Ba_{excess} = Ba_{measured} - [Al_{measured} \times (Ba/Al)_{detrital}] \quad (1)$$

where $Ba/Al_{detrital}$ is taken as the mean of the Ba/Al values observed above and below the S1 units. When Ba_{excess} is estimated in this manner, mean values of 0.0032 and 0.0037 are found for $(Ba/Al)_{detrital}$ in LC21 and MD90–917, respectively. These estimates might be expected to contain a small component of biogenic Ba associated with the finite C_{org} content outside the sapropels, and in fact Ba/Al values as low as 0.0019 have been measured elsewhere in E. Mediterranean sediments and applied for $(Ba/Al)_{detrital}$ some other sapropel investigations (Van Os et al., 1994; Wehausen and Brumsack, 1999). All these values are low by comparison with the Ba/Al value of 0.0073 derived from the Turekian and Wedepohl (1961) shale compilation, a value that is often assumed for $(Ba/Al)_{detrital}$ when calculating the biogenic Ba level for productivity studies (Ba_{bio}, calculated analogously to Ba_{excess} above). A low $(Ba/Al)_{detrital}$ ratio may be a provenance characteristic of the E. Mediterranean basin, and it is possible that Ba_{bio} may be underestimated because too high a $(Ba/Al)_{detrital}$ correction has been applied.

The Ba/Al profile shapes in these two cores are similar to those of C_{org} (Figs. 2 and 3; Mercone et al., 2000). This common two-lobed shape is, however, quite different from the ‘quasi-Gaussian’ shape of Ba/Al profiles observed in several other S1 units where C_{org} profiles have been modified by post-depositional oxidation. These previous investigations were on S1 units that had accumulated more slowly than the cores here and were located mainly in deeper water in the eastern half of the eastern Mediterranean basin (Thomson et al., 1995; van Santvoort et al., 1996; Thomson et al., 1999; Mercone et al., 2000). The

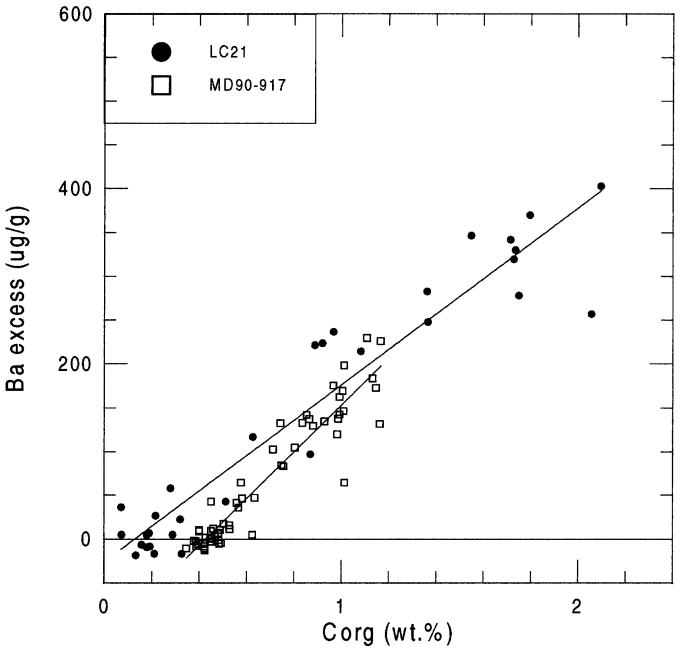

Fig. 4. Ba_{excess} versus C_{org} in cores LC21 and MD90–917, with y on x regression lines. Ba_{excess} is estimated as $Ba_{measured} - [Al_{measured} \times (Ba/Al)_{detrital}]$.

levels of Ba_{excess} as defined above, including the data from the light-coloured central sections, correlate well with C_{org} in both cores above a threshold C_{org} level of ~0.4 wt.% C_{org} (Fig. 4; Mercone et al., 2000). This initial correlation has been inferred but could not be demonstrated in earlier work (Thomson et al., 1995, 1999; van Santvoort et al., 1996).

The measured C_{org} contents must be less than those which were deposited because of C_{org} remineralization (see discussion of authigenic FeS_2 formation below), but it is less certain whether or not the Ba_{excess} values now observed were also higher at the time of deposition. The importance of dissolution and loss of Ba from barite in sediments was recognized and estimated to be ~30% by Dymond et al. (1992). Subsequent work has confirmed that Ba loss from sediments after deposition is widespread and substantial (McManus et al., 1994; 1998), and McManus et al. (1998) specifically concluded that Ba may be poorly preserved in the sediments under conditions of high C_{org} flux and low bottom water O_2 levels. This is a similar general description for the sea floor condition inferred above for S1 sapropel deposition from the micropalaeontological data. The C_{org}/Ba_{excess} ratio ($\mu g\ g^{-1}/\mu g\ g^{-1}$) now observed through the S1 sections in the two cores studied is 50–100, whereas observed values intercepted in sediment traps by Dymond and Collier (1996) were 33–50 ($Ba_{bio}/C_{org} \times 100 = 3\text{-}2$) in productive Pacific areas, and 33–20 ($Ba_{bio}/C_{org} \times 100 = 5\text{-}3$) in less productive areas. This sediment trap evidence is inconsistent with the present sediment data, because it is anticipated that C_{org}/Ba_{excess} ratios in the sediments would decrease if Ba_{excess} were preferentially preserved while C_{org} was remineralised. Although the uncertainties in the systematics of Ba uptake in the water column and dissolution in the sediments make it premature to use Ba_{bio} data to hindcast palaeoproductivity levels, the present data nevertheless lend credence to the use of Ba as a qualitative or possibly semi-quantitative indicator of sapropel C_{org} levels in situations where C_{org} oxidation has occurred.

3.3. Geochemical evidence: Mn

The Mn/Al profile shapes are quite different from those of the C_{org} and Ba/Al profiles, but the Mn/Al profiles in cores 90–917 and LC21 are closely similar

to each other (Figs. 2 and 3). In both cases there are: (a) low Mn/Al levels below the sapropels which continue into the lower lobes, (b) a small Mn/Al peak at the tops of the lower lobes and in the lower central sections, (c) lower Mn/Al values through the upper central sections which continue into the bases of the upper lobes, (d) a much larger second Mn/Al peak towards the tops of, but still within, the upper lobes and (e) smooth decreases in Mn/Al ratio with increasing distance above the sapropels. In core 90–917 the upper Mn peak is particularly large with maximum Mn values of >3 wt.%, while the corresponding maximum value in LC21 is 0.7 wt.% Mn.

Manganese responds to the reducing conditions developed in sediments by C_{org} remineralization (Calvert and Pedersen, 1993). In oxic sediments, Mn is present as a detrital phase and as authigenic oxyhydroxide phases. When such oxic sediments experience reduction on burial below the oxic zone, Mn oxyhydroxides are utilised as electron acceptors and Mn(IV) is reduced to soluble Mn(II). This Mn^{2+} diffuses in solution and may be re-oxidised to form diagenetic oxyhydroxides when oxic conditions are re-encountered in the surficial sediments. No Mn^{2+} is lost from the sediments in this situation when the overlying bottom waters are oxic, and instead at steady state a surficial sediment zone with a high Mn(IV) content will be maintained (Froelich et al., 1979).

In sediments deposited under an anoxic water column, Mn^{2+} from Mn(IV) reduction can be lost from the sediments to build up high Mn^{2+} contents in the overlying waters. It might be expected, therefore, that sedimentary Mn will exist only at detrital levels under anoxic water columns, and indeed the most recent deep Black Sea sediments have a low Mn content (<500 $\mu g\ g^{-1}$) and high Mn contents in the anoxic-sufidic water column (Calvert and Pedersen, 1993). Huckriede and Meischner (1996) have shown, however, that layers of very high Mn content occur in deep Baltic Sea basins in which the bottom waters are also generally anoxic sulfidic. These Mn-rich layers are produced as a result of brief episodes of bottom water oxygenation, where the Mn is first precipitated when the water column is re-oxygenated, and then subsequently and rapidly converted from the precipitated Mn(IV) oxyhydroxides to the mixed [Ca,Mn(II),Mg] carbonate kutnahorite at the sediment water interface after anoxic bottom water conditions are re-established. The preferential settling of Mn oxyhydroxides in the deeper parts of the basin results in the apparent anomaly of high mean Mn contents in the sediments of deeper Baltic anoxic-sulfidic basins with Mn depletion in adjacent shallower, anoxic non-sulfidic marginal areas (Huckriede and Meischner, 1996).

In the case of core LC21 where micropaleontological data are available, both Mn/Al peaks correspond to the times when *G. orbicularis* appears as the dominant benthic foraminifer at the expense of the ODS species tolerant of near anoxia (Figs. 1 and 2). The mechanism for the formation of the two Mn/Al peaks in both cores is therefore interpreted as being related to times when O_2 levels increased in the bottom waters. It was deduced from the benthic micropalaeontological data that bottom waters were probably not anoxic sulfidic during S1 formation, but they may still have been sufficiently anoxic to receive Mn^{2+} from the sediments (Thomson et al., 1995). Escape from the sediments to the water column, followed by precipitation at times of increased reventilation and bottom water O_2 content, as inferred from the micropaleontological data, would explain the occurrence of two peaks. Preferential deposition of the flocculated Mn oxyhydroxide from the water column in local pockets would also explain the variable magnitude of the upper Mn peaks. Both upper Mn peaks occur just before the end of S1 formation as defined by the C_{org} and Ba/Al profiles returning to baseline values. On this explanation, it is unlikely that the Mn peaks in these cores can be stable at present as Mn oxyhydroxides, because they are all too deep in these cores to be experiencing oxic conditions at the present time. The two smaller lower peaks in particular must have been in anoxic conditions for ~6 ky. The largest Mn peak around 227 cm in core 90–917 with a maximum content of ~3.3 wt.% is exactly coincident with increases of both $CaCO_3$ (+7 wt.% local increase in $CaCO_3$) and Mg (+10% local increase relative to Al; Fig. 3). The presence of kutnahorite in the samples with highest Mn contents is also confirmed by the characteristic X-ray diffraction d-spacing peak at 2.94 Angstrom that is not present in surrounding samples. Although the remaining three Mn peaks are too small to affect the bulk sediment Ca and Mg profiles, it is likely they are now also present in the form of kutnahorite.

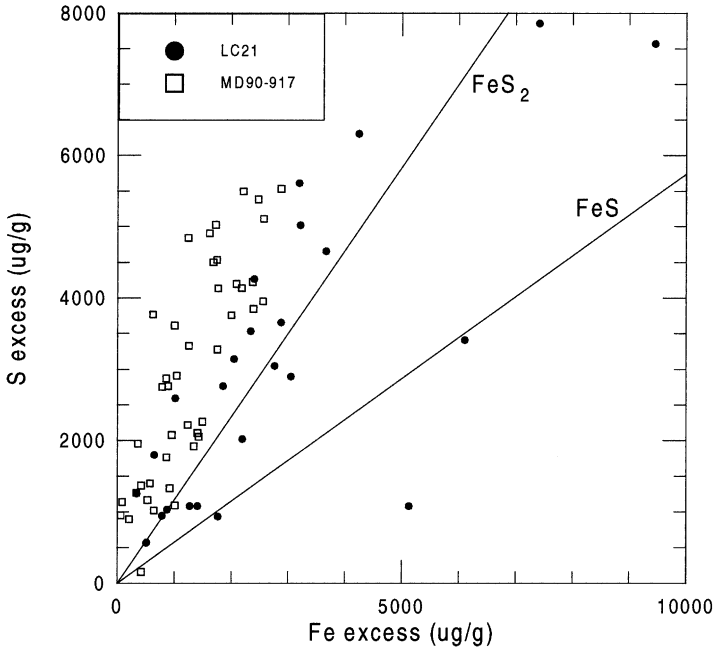

Fig. 5. S_{excess} versus Fe_{excess} in cores LC21 and MD90–917, with the stoichiometric lines FeS and FeS_2. S_{excess} is estimated as $S_{measured} - [Cl_{measured} \times (S/Cl)_{seawater}]$, while Fe_{excess} is $Fe_{measured} - [Al_{measured} \times (Fe/Al)_{detrital}]$.

This interpretation of reventilation at the end of S1 times to form the upper Mn peaks observed in cores 90–917 and LC21 is similar to that proposed for the upper of two Mn peaks observed in most S1 sapropels investigated to date (Higgs et al., 1994; Thomson et al., 1995, 1999; van Santvoort et al., 1996). The explanation here for the lower peak in the central sections is different from that for the lower peak in slower-accumulated cores, however. In those cases the lower peaks have been caused by the downwards progression of an oxidation front which has operated since the reventilation at the end of S1 times, and both peaks have been proved to be in oxic conditions in these cores (van Santvoort et al., 1996).

3.4. Geochemical evidence: S

Like C_{org} and Ba/Al, S exhibits a double-lobed profile in both cores (Figs. 2 and 3). Sulfur enrichment in organic-rich marine sediments is mainly developed after deposition by the formation of FeS_2 (pyrite) following anoxic sulfidic remineralization of sedimentary C_{org} by SO_4^{2-} (Berner, 1970, 1984):

$$C_{106}H_{263}O_{110}N_{16}P + 53SO_4^{2-} \rightarrow 106CO_2 + 16NH_3 + H_3PO_4 + 53S^{2-} + 106H_2O \quad (2)$$

The production route to FeS_2 in sediments is complex, but is believed to occur through the progressive reaction of polysulfides or S(0) with precursor Fe monosulfides formed from Fe^{2+} in the sediments or pore waters, in the sequence mackinawite (Fe_9S_8) → greigite (Fe_3S_4) → pyrite (Wilkin and Barnes, 1996).

Sulfur has an appreciable concentration in sea water as SO_4^{2-}, so that S_{excess} in the sediments is defined by a correction relative to Cl to account for the pore water salt contribution:

$$S_{excess} = S_{measured} - [Cl_{measured} \times (S/Cl)_{seawater}] \quad (3)$$

where $(S/Cl)_{seawater} = 0.905/19.355$. A plot of S_{excess} versus Fe_{excess} (Fig. 5) illustrates that S_{excess} in both cores consistently exceeds the stoichiometries of FeS and FeS_2. By means of selective S-speciation

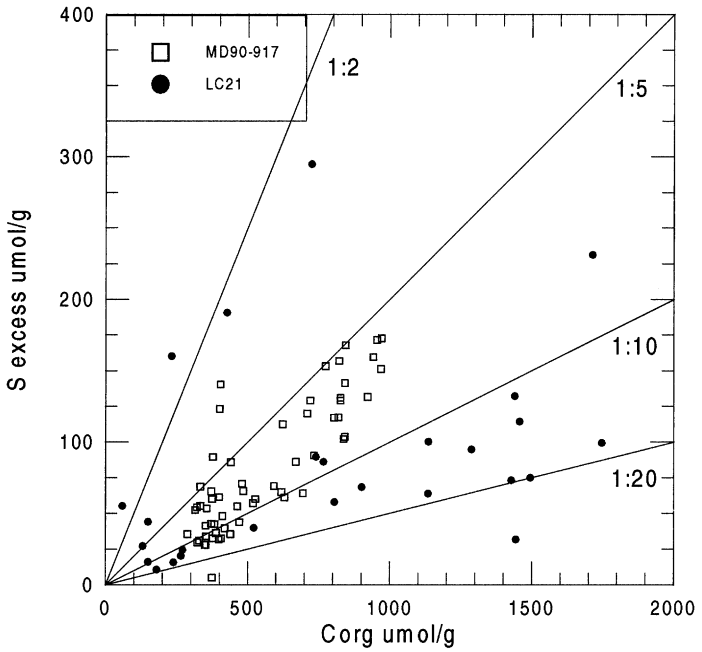

Fig. 6. Molar S_{excess} versus molar C_{org} in cores LC21 and MD90–917, with lines of various slopes as indicated.

leaching techniques, Passier et al. (1998) demonstrated that pyrite S was the dominant form of S in other eastern Mediterranean S1 units. Besides FeS_2 and sea salt SO_4^{2-}, the abundance of other forms of S was in the sequence:

humic S $\gg$ polysulfide S $>$ S(0) $>$ acid volatile S.

The additional S_{excess} over that required to form FeS_2 in the cores studied is therefore likely to be present in organo-S associations. The S profiles, including higher S values in the central sections, all of which are secondary, have similarities in shape to the profiles of C_{org} and Ba that have a depositional origin. It was inferred earlier that bottom water conditions during formation of the central sections probably had an increased O_2 level, and such conditions would not have allowed sulfide formation at the sediment water interface. It follows that sulfide formation in the central sections must either have occurred under a thin oxic zone, or later when the upper S1 lobe was being deposited.

The S_{excess} data may be expressed alternatively in terms of the amount of C_{org} originally deposited which has been remineralised by SO_4^{2-} in the sediments. Noting that 2 moles of C_{org} are required to form 1 mole of S as S^{2-}, 15–30% (between the 1:10 and 1:5 lines of Fig. 6) of the initial C_{org} is now present in MD90–917 as sulfide, and 10–15% (between the 1:20 and 1:10 lines) has been consumed in LC21. These figures overlap with values previously determined for S1 (20–45%; Passier et al., 1999), but all such estimates of C_{org} consumed must be viewed as minima because reduced S can be re-oxidised after formation and lost from the sediments as SO_4^{2-} (Canfield and Teske, 1996). A few S_{excess} data points suggest a higher utilization of C_{org} (Fig. 6) but these samples are from the bases of the lower lobes. Passier et al. (1996) have demonstrated that a grey halo develops below some sapropel units in which S^{2-} generation exceeds the locally-available Fe^{2+}. This grey coloration was ascribed to diagenetic pyrite formation where S^{2-} which had diffused downwards out of the S1 unit encountered an upwards Fe^{2+} flux from deeper anoxic horizons (Passier et al., 1996). On the evidence that no grey halo was formed in either core studied, pyrite production is inferred not to have been Fe limited in these two S1 examples, but the high S values towards the bases of the lower lobes probably represent such a reaction with the Fe flux from below (Figs. 2 and 3).

The relationships developed between sedimentary

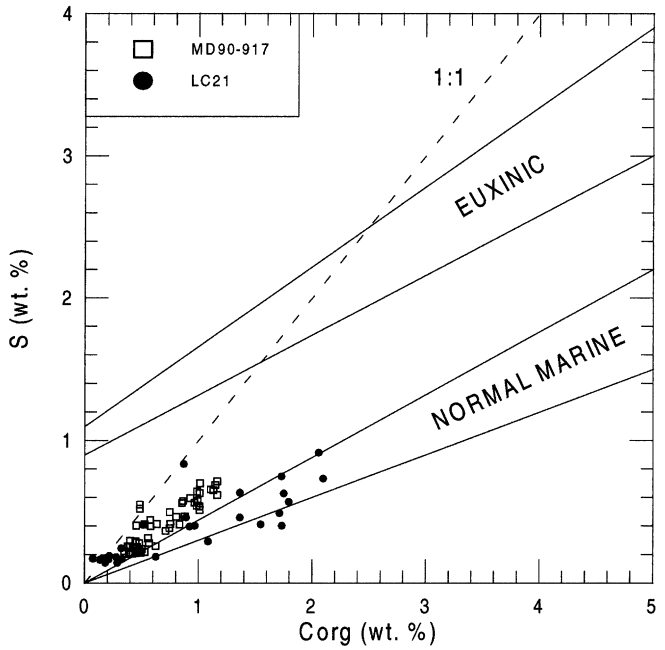

Fig. 7. Sulfur (total) versus C_{org} in cores LC21 and MD90–917. The isoline and domains for sediments inferred to have been deposited under euxinic and oxic water columns are indicated (Leventhal, 1995).

C_{org} contents and syndepositional and diagenetic pyrite are sufficiently characteristic that they have been used as criteria to define the oxidation status of the overlying water column at the time of sediment deposition (Berner, 1970; Berner and Raiswell, 1984; Raiswell and Berner, 1986; Lyons and Berner, 1992). Although special situations have been identified where S/C plots are equivocal (Leventhal, 1995), the critical difference between deposition under an anoxic-sulfidic water column and under normal marine conditions with an oxic water column is that extra S deposited directly from euxinic water columns results in a domain well above the oxic domain on a S/C plot. On S/C criteria, all the data from the cores here plot in or just above the normal marine domain (Fig. 7). Raiswell et al (1988)also showed that Degree of Pyritization (DOP = [pyritic Fe]/[pyritic Fe + acid-soluble Fe]) values <0.42 were characteristic of sediments deposited in aerobic conditions while values >0.55 were characteristic of sediments deposited under anoxic-sulfidic water columns. Although Fe speciation measurements are not available for the cores investigated, Passier et al. (1996) have suggested the use of DOP_T as an approximation to DOP, where DOP_T is the molar ratio 0.5.S/Fe. DOP_T values for core 90–917 do not exceed 0.15, and those for core LC21 do not exceed 0.25. By analogy with known situations, therefore, the C_{org}, Fe and S data from cores 90–917 and LC21 do not indicate that the overlying water column was anoxic-sufidic during S1 formation. This is consistent with the benthic foraminiferal data, where the intermittent presence of ODS species through both S1 lobes is similarly inconsistent with continuous anoxic-sulfidic bottom water conditions.

3.5. Redox-sensitive element enrichments: As, Cr, Cu, Mo, Ni, Se, U, V and Zn

Like C_{org}, Ba and S, many redox-sensitive elements exhibit double peaks in their concentration versus depth profiles through S1 (Figs. 8 and 9). In Tables 1 and 2, the mean element contents of the S1 units (including the lighter-coloured central sections) are compared with the means of the over- and underlying sediments. Elemental excesses in S1 have been estimated by subtracting the detrital contents projected from the measured Al content, a procedure that

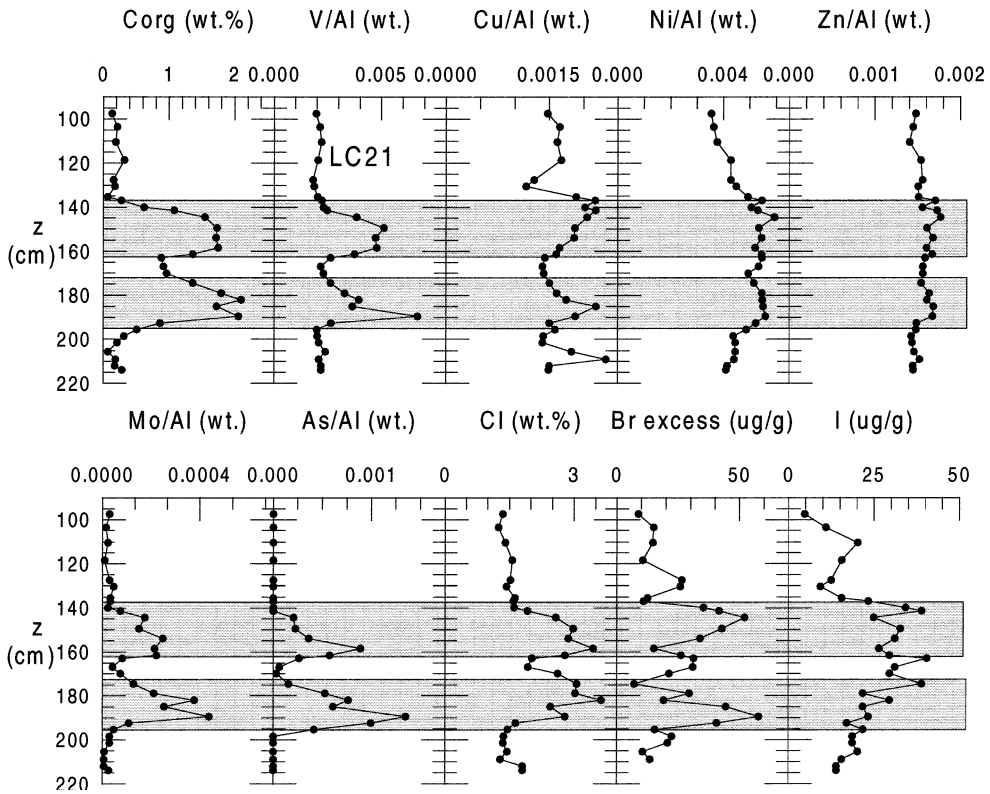

Fig. 8. Concentration (C_{org} and Cl wt.%, Br and I, $\mu g\ g^{-1}$) and Al-normalised concentration (V, Cu, Ni, Zn, Mo and As) versus depth profiles for core LC21. Br_{excess} is estimated as $Br_{measured} - [Cl_{measured} \times (Br/Cl)_{seawater}]$. The two dark coloured lobes in S1 are shaded.

assumes that the detrital component in the sapropel has the same composition as the surrounding sediments. This procedure is substantiated by the generally similar levels calculated for the major elements (except Mn and Fe for reasons discussed above) and for minor elements which do not have an authigenic enrichment (Ce, La, Nb, Pb, Th, Y and Zr). Many of the minor elements often identified as being enriched in sapropels or black shales (i.e. As, Cr, Cu, Mo, Ni, Se, U, V and Zn) emerge from this analysis in both cores, although the enrichments are modest for a sapropel (Calvert, 1983; Nijenhuis et al., 1999). All elemental enrichments are greater in LC21 than in MD90–917, because of the higher accumulation rate and lower C_{org} and S contents of the latter. The detrital values of Ni and Cr in both cores are high relative to shale values. High concentrations of these two elements along with Mg are diagnostic of ultrabasic or basic rocks (Turekian and Wedepohl, 1961), and the high Ni and Cr values may represent a contribution of detrital phases from the southern European Tethyan ophiolite belt to these sediments. Bromine and I show enrichments by the procedure adopted in Table 1, and these elements generally have well-established associations with C_{org} in organic-rich sediments (Price and Calvert, 1977; Shimmield and Pedersen, 1990), including sapropels (Ten Haven et al., 1987). In cores 90–917 and LC21, however, there is a correlation of Cl with C_{org} that probably arises from the higher porosity of the C_{org}–rich S1 sediments (Figs. 8 and 9). Assuming that the measured Cl is all from seawater salt, the salt-corrected Br and (total) I profiles confirm a small enrichment in these low C_{org} S1 units.

Four principal routes by which C_{org}-rich sediments develop high authigenic levels of redox-sensitive elements have been identified (Calvert and Pedersen, 1993; Piper, 1994; Wignall, 1994):

1. A pre-concentration in the water column by

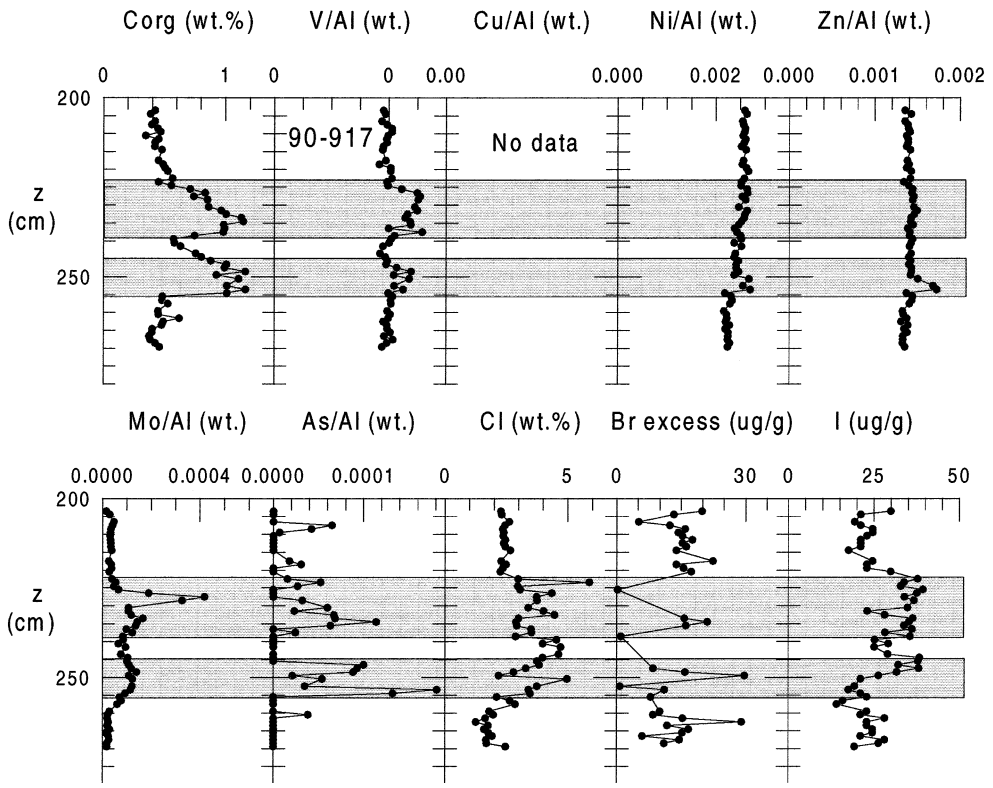

Fig. 9. Concentration (C_{org}, S and Cl wt.%, Br and I μg g^{-1}) and Al-normalised concentration (V, Ni, Zn, Mo and As) versus depth profiles for core MD90–917. Br_{excess} is estimated as $Br_{measured} - [Cl_{measured} \times (Br/Cl)_{seawater}]$. The two dark coloured lobes in S1 are shaded.

biological uptake before deposition, with settling to the sediment/water interface. Organic uptake followed by remineralization in the water column is believed to be the cause of the observed similarities in sea water concentration versus depth profiles between the minor elements Cu, Ni and Zn and the nutrients HPO_4^{2-} and $Si(OH)_4$ (Bruland, 1983). Deposition with C_{org} has been invoked for Ba, Cr, Cu, Mo, Ni, U, V and Zn (Piper, 1994), although there is considerable uncertainty on the relative importance of this mechanism for different elements because of the variable elemental contents observed in plankton analyses (Collier and Edmond, 1984; Brumsack, 1986).

2. For an anoxic-sulfidic water column only, sulfide formation and settling Fe and Mn sulfides in the water column can transport other elements to the sediment/water interface. The chalcophile elements Cu, Ni and Zn may be precipitated as sulfides in this way without undergoing a valency change (Emerson and Huested, 1991), and reduced Mo is also believed to be supplied to the sediments in this manner (Piper, 1994).
3. Diffusion from seawater through pore waters to a depth in the sediments where a sufficiently low redox potential exists to promote a valency change. This mechanism is effective where bottom waters are oxic but sediments are anoxic-non-sulfidic or anoxic-sulfidic at shallow depth. The elements Cr, Mo, U and V are believed to be enriched in this way by precipitation under anoxic conditions with a reductive valency change (Calvert and Pedersen, 1993; Crusius et al., 1996).
4. A combination mechanism of (1) or (2) with (3), by which an element originally delivered to the sediment/water interface with settled organic material is subsequently released and is reduced or complexed with C_{org} or sulfide on downwards

Table 1
Compositional comparison of S1 unit with enclosing sediments in Aegean Sea core LC21.

Element or element/Al ratio	B'gnd mean 97–137 cm and 198–214 cm	B'gnd mean, std. dev.	S1 mean, 140–196 cm	S1 mean, std. dev.	S1/ b'gnd ratio	S1/b'gnd ratio, std. dev.	Excess element in S1 (μg/g)	B'gnd mean element content (μg/g cfb)[a]	S1 mean element content (μg/g cfb)[a]	Element shale content (μg/g)	Element seawater content (μg/l)	Equivalent seawater volume (l)
Corg wt.%	0.20	0.08	1.35	0.50	6.76	3.69	11528					
CaCO3 wt.%	47.27	3.25	41.65	2.17	0.88	0.08						
Si/Al	3.15	0.11	3.15	0.05	1.00	0.04	3221	240374	222742	273000		
Al wt.%	4.02	0.30	4.13	0.23	1.03	0.10	0	76190	70727	80000		
Ti/Al	0.054	0.001	0.054	0.002	0.98	0.03	20	4151	3786	4600		
Fe/Al	0.63	0.05	0.70	0.05	1.11	0.12	3613	48138	49692	47200		
Mn/Al	0.030	0.018	0.049	0.049	1.62	1.91	798	2284	3432	850		
Mg/Al	0.72	0.02	0.72	0.03	1.00	0.05	854	54883	51061	[15000]		
CaO	26.24	1.71	23.71	1.09	0.90	0.07				[22100]		
K/Al	0.046	0.019	0.055	0.019	1.21	0.65	452	3479	3919	26600		
P/Al	0.010	0.001	0.010	0.001	1.05	0.16	30	761	739	700		
Cl wt.%	1.48	0.18	2.52	0.65	1.70	0.48	10364				19353000	0.0005
S wt.%	0.17	0.02	0.53	0.20	3.05	1.22	3539				905000	0.0039
As/Al	0	0	0.00035	0.00031			14	0	25	13	2	7
Ba/Al	0.0032	0.0006	0.0092	0.0026	2.93	0.97	254	240	653	580	11.7	22
Br ppm	64	8	119	24	1.87	0.43	55	121	205	4	67000	0.0008
Ce/Al	0.0011	0.0002	0.0009	0.0001	0.88	0.16	−4	80	66	59		
Cr/Al	0.0043	0.0003	0.0049	0.0002	1.13	0.09	28	328	345	90	0.33	86
Cu/Al	0.0016	0.0003	0.0017	0.0003	1.06	0.27	6	125	123	45	0.12	50
I ppm	15	5	29	7	1.91	0.76	14	29	50	2	60	0.23
La/Al	0.00046	0.00006	0.00045	0.00006	0.96	0.17	0	35	32	92		
Mo/Al	0.00002	0.00001	0.00017	0.00012	7.3	6.3	6	2	12	2.6	11	0.5
Nb/Al	0.00026	0.00001	0.00024	0.00001	0.94	0.05	0	20	17	11		
Ni/Al	0.00431	0.00050	0.00534	0.00025	1.24	0.16	47	328	378	68	0.48	98
Pb/Al	0.00031	0.00004	0.00027	0.00002	0.88	0.12	−1	24	19	20		
Se/Al	0.000002	0.000003	0.000064	0.000037	31	52	3	0	5	0.6	0.17	15
Sr ppm	730	35	766	69	1.05	0.11	35	1385	1312	[300]		
Th/Al	0.00011	0.00003	0.00011	0.00001	0.93	0.23	0	9	8	12		
U/Al	0.00006	0.00002	0.00014	0.00004	2.34	1.13	3	5	10	3.7	3.20	1
V/Al	0.0021	0.0001	0.0035	0.0013	1.66	0.63	59	159	245	130	1	59
Y/Al	0.00038	0.00002	0.00039	0.00001	1.02	0.05	1	29	28	26		
Zn/Al	0.0015	0.0001	0.0016	0.0001	1.08	0.08	7	114	114	95	0.39	17
Zr/Al	0.0019	0.0001	0.0018	0.0000	0.94	0.04	−2	148	129	160		

[a] cfb = carbonate free basis; elemental shale data from Turekian and Wedepohl, 1961.

Table 2
Compositional comparison of S1 unit with enclosing sediments in Adriatic Sea core 90–917.

Element or element/Al ratio	B'gnd mean, 203–223 cm and 256–270 cm	B'gnd mean, std. dev.	S1 mean, 224–256 cm	S1 mean, std. dev.	S1/b'gnd ratio	S1/b'gnd ratio, std. dev.	Excess element in S1 (μg/g)	B'gnd mean element content (μg/g cfb)[a]	S1 mean element content (μg/g cfb)[a]	Element shale content (μg/g)	Element seawater content (μg/l)	Equivalent seawater volume (l)
Corg wt.%	0.45	0.06	0.86	0.21	1.92	0.52	4122					
CaCO3 wt.%	29.36	1.38	29.14	2.45	0.99	0.10						
Si/Al	2.87	0.02	2.83	0.06	0.99	0.02	−4758	240895	233433	273000		
Al wt.%	5.94	0.06	5.84	0.27	0.98	0.05	−1015	84055	82362	80000		
Ti/Al	0.049	0.001	0.047	0.001	0.97	0.03	−149	4127	3904	4600		
Fe/Al	0.59	0.02	0.61	0.01	1.04	0.03	879	49519	50606	47200		
Mn/Al	0.025	0.010	0.084	0.149	3.40	6.20	3430	2075	6909	850		
Mg/Al	0.55	0.01	0.54	0.03	0.99	0.06	−1007	45893	44329	[15000]		
CaO	16.84	0.28	16.14	0.63	0.96	0.04				[22100]		
K/Al	0.18	0.01	0.16	0.02	0.90	0.14	−1191	14715	12990	26600		
P/Al	0.0075	0.0004	0.0077	0.0010	1.03	0.15	4	633	636	700		
Cl wt.%	2.18	0.40	3.64	0.81	1.67	0.48	14639				19353000	0.0008
S wt.%	0.27	0.09	0.51	0.13	1.85	0.77	2318				905000	0.0026
As/Al	0.000007	0.000016	0.000040	0.000047	5.64	14.56	2	1	3	13	2	1
Ba/Al	0.0037	0.0001	0.0057	0.0010	1.56	0.27	116	308	471	580	11.7	10
Br ppm	87	13	114	10	1.31	0.23	27	123	160	4	67000	0.0004
Cr/Al	0.0029	0.0001	0.0030	0.0001	1.01	0.06	−1	247	245	90	0.33	−3
I ppm	22	3	31	6	1.38	0.35	9	32	44	2	60	0.1
Mo/Al	0.000033	0.000015	0.000119	0.000077	3.64	2.90	5	3	10	2.6	11	0.5
Ni/Al	0.0024	0.0002	0.0025	0.0001	1.04	0.09	3	203	206	68	0.48	6
Pb/Al	0.00029	0.00008	0.00038	0.00016	1.32	0.67	5	24	31	20		
Rb/Al	0.00166	0.00003	0.00170	0.00004	1.02	0.03	1	140	140	140		
Sr ppm	428	31	433	21	1.01	0.09	6	605	611	[300]		
Th/Al	0.00012	0.00001	0.00013	0.00001	1.07	0.11	0	10	10	12		
U/Al	0.00001	0.00001	0.00003	0.00001	1.94	1.65	1	1	2	3.7	3.2	0.2
V/Al	0.0020	0.0001	0.0022	0.0002	1.11	0.12	11	166	180	130	1	11
Y/Al	0.00030	0.00001	0.00028	0.00002	0.94	0.06	−1	25	23	26		
Zn/Al	0.00137	0.00003	0.00144	0.00008	1.05	0.06	3	115	119	95	0.39	7
Zr/Al	0.00125	0.00004	0.00123	0.00010	0.98	0.08	−3	105	101	160		

[a] cfb = carbonate free basis; elemental shale content data from Turekian and Wedepohl, 1961.

diffusion. Such an interfacial release has the effect of increasing the flux of an element over that possible by downwards diffusion from bottom waters alone, and the effects of this process have been demonstrated for Cu (Boyle et al., 1977; Shaw et al., 1990). Huerta-Diaz and Morse (1992) have shown that As, Co, Cu, Mn, Mo and Ni develop high concentrations in pyrite at the expense of the precursor sediments. The poor preservation of biogenic silica in E. Mediterranean sediments (Schrader and Matherne, 1981; Kemp et al., 1999) means that any elements initially deposited with opal may be released in this way.

Judging the relative magnitudes of authigenic enrichments (Tables 1 and 2) has to take into account the variable magnitudes of the detrital aluminosilicate contents. A 10 $\mu g\ g^{-1}$ authigenic enrichment of Mo, for example, is readily identified because background shale Mo contents are ~2–3 $\mu g\ g^{-1}$, whereas a similar enrichment for V must be identified against a detrital V content of 159–166 $\mu g\ g^{-1}$ (Tables 1 and 2). Calculated enrichments ($\mu g\ g^{-1}$) have therefore been expressed alternatively in terms of the number of litres of seawater that would have to be quantitatively stripped of an element to produce that element's observed authigenic enrichment. It is implicit in this procedure that the elemental enrichments are considered to be derived entirely from seawater rather than by an alternative mechanism such as hydrothermal input or diagenetic supply from surrounding sediments. The equivalent volume of seawater calculation does not imply a common uptake mechanism, however. Even if all elements were enriched by mechanisms (3) and (4) above, each element would develop its authigenic enrichment by a characteristic diffusive path length and concentration gradient from the sediment/water interface to the depth of immobilization.

For core LC21 the order of enrichment of the elements in $\mu g\ g^{-1}$ is (Table 1):

$$59 = V > Ni > Cr > As > 10 > Zn > Mo = Cu > Se = U = 3$$

which in equivalent seawater volumes (litres) corresponds to an order:

$$100 > Ni > Cr > V > Cu > Zn > Se > 10 > As > U > 1 > Mo.$$

The maximum enrichment in core MD90–917 is for V at 11 $\mu g\ g^{-1}$, equivalent to 11 l of sea water (Table 2). In both cores the calculated Ba_{excess} is greater than that for V_{excess} or any other element, although the equivalent volumes of sea water are greater or similar for Cr, Cu, Ni, V and Zn. In core LC21, the equivalent volumes of seawater for the observed enrichments are 100–10 l for Ba, Cu, Cr, Ni, Se, V and Zn, 10-1 l for As and U and <1 l for Mo. By analogy with the known behaviour of Ba, it may be that the first group of elements represents those deposited along with C_{org} or other biogenic component, while the smaller equivalent volumes of Mo and U might be developed by diffusion into the sediments from bottom waters (Crusius et al., 1996).

Nijenhuis et al. (1999) have reported the geochemical analysis of a Pliocene sapropel (i-282) which has very high C_{org} contents (average 13.1%, maximum 27.3%) and elemental enrichments. In that unit the observed order of mean elemental enrichment in terms of abundance ($\mu g\ g^{-1}$) is:

$$1206 = V > Mo > Ni > Cu > 100 > Cr > As > Se > Zn = 21,$$

whereas the sequence in terms of equivalent sea water volumes is:

$$1250 = Cu > V > 1000 > 500 > Ni > Cr > Se > 100 > Zn > As > Mo = 23$$

Sapropel i-282 contains isorenieratene derivatives, which are believed to be derived solely from photosynthetic green S bacteria (Nijenhuis et al., 1999). The presence of isorenieratene derivatives is therefore interpreted to imply an anoxic-sulfidic condition in the lower photic zone. The unit is also laminated, which implies an anoxic-sulfidic sea floor with no bioturbation, so that the evidence is that i-282 formed under an euxinic water column with only a shallow (<200 m?) surficial oxic layer.

Despite the difference between the inferred water column conditions during formation of sapropel I-282

and S1, and the very large elemental enrichments in i-282 relative to S1, the same group of elements is enriched in both. The mean C_{org} content in i-282 is ×10 greater than the mean C_{org} content of S1 in LC21, and the only elements for which the i-282/LC21 ratios ($\mu g\ g^{-1}/\mu g\ g^{-1}$) exceed10 are Mo (×471) and V (×21). These are the two elements with the most extreme enrichments in sediments that have formed under an anoxic sulfidic water column (Emerson and Huested, 1991; Piper, 1994), although the mechanism for the removal of the two elements appears to be different. Wanty and Goldhaber (1992) expect that high concentrations of dissolved sulfide reduce the V(V) species found in oxic sea water to the V(III) forms V_2O_3 or $V(OH)_3$, while Mo may be reduced from Mo(VI) species to the insoluble Mo(IV) phase MoS_2 (Emerson and Huested, 1991). This compositional comparison is therefore also consistent with less reducing water column conditions at the time of S1 formation than the anoxic sulfidic conditions during i-282 formation.

4. Conclusions

A parallel investigation of foraminiferal micropaleontology and geochemistry of rapidly-accumulated sediments in two cores from the Adriatic and Aegean Seas provides evidence of changes in bottom water oxygenation levels through the deposition of the S1 sapropel in these areas. Bottom water conditions were generally severely dysoxic but probably not anoxic-sulfidic during the formation of sapropel S1, but both cores display a brief phase of improved bottom water oxygenation in the middle of S1 times. This interpretation derives from the benthic foraminiferal record and the solid phase Mn record. The improved ventilation episode also coincided with a surface ocean cooling indicated by the planktonic foraminiferal record and a lessening in productivity indicated by the S1 Ba/Al record. Although high deposition rates have diluted the S1 C_{org} values to low levels, the same suite of redox-sensitive elements is found to be enriched as in most other S1 units, older sapropels and black shales. By analogy with Ba which has a close correspondence with C_{org}, many of these elements (Cu, Cr, Ni, Se, V and Zn) are inferred to have been supplied to the sediments along with C_{org}, but others (S, Mo and U) appear to have developed in the sediments after deposition. By comparison with the metal enrichments observed in an older sapropel which appears to have been deposited under a water column which was anoxic-sulfidic to near the ocean surface, only the elements Mo and V are relatively more enriched than C_{org} in the older sapropel than in these S1 examples. Very high contents of these two elements may be diagnostic of an anoxic-sulfidic water column.

Acknowledgements

We are grateful to IFRTP for the recovery of both cores from their vessel *Marion Dufresne*, and to Dr Martine Paterne for guidance on core selection and provision of samples from core MD90–917. This work was partly supported by the EU Marine Science and Technology SAP (MAS3-CT97-0137) and CLIVAMP (MAS3-CT95-0043) programmes. We thank Mr T. Clayton for comparative XRD analyses on core 90–917 samples, and Drs S. Calvert and R. Wehausen for helpful formal reviews of the original version of the script.

References

Berner, R.A., 1970. Sedimentary pyrite formation. Amer. J. Sci. 268, 1–23.

Berner, R.A., 1984. Sedimentary pyrite formation: an update. Geochim. Cosmochim. Acta 48, 605–615.

Berner, R.A., Raiswell, R., 1984. Burial of organic carbon and pyrite sulfur in sediments over Phanerozoic time: a new theory. Geochim. Cosmochim. Acta 47, 855–862.

Bruland, K.W., 1983. Trace elements in seawater. In: Riley, J.P., Chester, R. (Eds.), Chemical Oceanography, Vol. 8. Academic Press, London, pp. 157–220.

Bethoux, J.-P., Pierre, C., 1999. Mediterranean functioning and sapropel formation: respective influences of climate and hydrological changes in the Atlantic and the Mediterranean. Mar. Geol. 153, 29–39.

Boyle, E.A., Sclater, F.R., Edmond, J.M., 1977. The distribution of dissolved copper in the Pacific. Earth Planet. Sci. Lett. 37, 38–54.

Brumsack, H.-J., 1986. The inorganic geochemistry of Cretaceous black shales (DSDP Leg 41) in comparison to modern upwelling sediments from the Gulf of California. In: Summerhayes, C.P., Shackleton, N.J. (Eds.), North Atlantic Paleoceanography Geol. Society London, Spec. Publ. 21, 447–462.

Calvert, S.E., 1983. Geochemistry of Pleistocene sapropels and associated sediments from the Eastern Mediterranean. Oceanol. Acta 6, 255–267.

Calvert, S.E., Pedersen, T.F., 1993. Geochemistry of Recent oxic and anoxic marine sediments: implications for the geological record. Mar. Chem. 113, 67–87.

Canfield, D.E., Teske, A., 1996. Late Proterozoic rise in atmospheric oxygen concentration inferred from phylogenetic and sulfur-isotope studies. Nature 382, 127–132.

Castradori, D., 1993. Calcareous nannofossils and the origin of eastern Mediterranean sapropels. Paleoceanography 8, 459–471.

Cita, M.B., Grignani, D., 1982. Nature and origin of Late Neogene Mediterranean sapropels. In: Schlanger, S.O., Cita, M.B. (Eds.), Nature and Origin of Cretaceous Carbon-Rich Facies. Academic, San Diego, California, pp. 165–196.

Cita, M.B., Vergnaud-Grazzini, C., Robert, C., Chamley, H., Ciaranfi, N., Donofrio, S., 1977. Paleoclimatic record of a long deep-sea core from the eastern Mediterranean. Quaternary Research 8, 205–235.

Collier, R., Edmond, J.M., 1984. The trace element geochemistry of marine biogenic particulate matter. Prog. Oceanogr. 13, 113–199.

Crusius, J., Calvert, S., Pedersen, T., Sage, D., 1996. Rhenium and molybdenum enrichments in sediments as indicators of oxic, suboxic and sulfidic conditions of deposition. Earth Planet. Sci. Lett. 145, 65–78.

De Lange, G.J., Middelburg, J.J., Pruysers, P.A., 1989. Discussion: Middle and Late Quaternary depositional sequences and cycles in the eastern Mediterranean. Sedimentology 36, 151–156.

De Rijk, S., Hayes, A., Rohling, E.J., 1999. Eastern Mediterranean sapropel S1 interruption: an expression of the onset of climatic deterioration around 7 ka BP. Mar. Geol. 153, 337–343.

Dymond, J., Collier, R., 1996. Particulate barium fluxes and their relationships to biological productivity. Deep-Sea Res. II 43, 1283–1308.

Dymond, J., Suess, E., Lyle, M., 1992. Barium in deep-sea sediment: A geochemical proxy for paleoproductivity. Paleoceanography 7, 163–181.

Emeis, K.-C., and the Shipboard Scientific Party, 1996. Paleoceanography and sapropel introduction. In Emeis, K.C., Robertson, A.H.F., Richter, C. (Eds.), Proc. ODP, Init. Repts. 160, 21–28.

Emerson, S.R., Huested, S.S., 1991. Ocean anoxia and the concentrations of molybdenum and vanadium in seawater. Mar. Chem. 34, 177–198.

Fontugne, M.R., Calvert, S.E., 1992. Late Pleistocene variability of the organic carbon isotopic composition of organic matter in the eastern Mediterranean: monitor of changes in organic carbon sources and atmospheric CO_2 concentrations. Paleoceanography 7, 1–20.

Francois, R., Honjo, S., Manganini, S.J., Ravizza, G.E., 1995. Biogenic barium fluxes to the deep sea: Implications for paleoproductivity reconstruction. Global Biogeochem. Cycles 9, 289–303.

Froelich, P.N., Klinkhammer, G.P., Bender, M.L., Luedtke, N.A., Heath, G.R., Cullen, D., Dauphin, P., 1979. Early oxidation of organic matter in pelagic sediments of the eastern equatorial Atlantic, suboxic diagenesis. Geochim. Cosmochim. Acta 43, 1075–1090.

Hieke, W., 1976. Problems of eastern Mediterranean Late Quaternary stratigraphy—a critical re-evaluation of the literature. 'Meteor' Forschungsergeb. Reihe C 24, 68–88.

Higgs, N.C., Thomson, J., Wilson, T.R.S., Croudace, I.W., 1994. Modification and complete removal of eastern Mediterranean sapropels by postdepositional oxidation. Geology 22, 423–426.

Hilgen, F.J., 1991. Astronomical calibration of Gauss to Matuyama sapropels in the Mediterranean and implication for the geomagnetic polarity time scale. Earth Planet. Sci. Lett. 104, 226–244.

Huckriede, H., Meischner, D., 1996. Origin and environment of manganese-rich sediments within black-shale basins. Geochim. Cosmochim. Acta 60, 1399–1413.

Huerta-Diaz, M.A., Morse, J.W., 1992. Pyritization of trace metals in anoxic marine sediments. Geochim. Cosmochim. Acta 56, 2681–2702.

Jorissen, F.J., 1999. Benthic foraminiferal successions across Late Quaternary Mediterranean sapropels. Mar. Geol. 153, 91–101.

Jorissen, F.J., Asioli, A., Borsetti, A.M., Capotondi, L., de Vischer, J.P., Hilgen, F.J., Van der Borg, K., Vergnaud-Grazzini, C., Zachariasse, W.J., 1993. Late Quaternary central Mediterranean biochronology. Mar. Micropaleontol. 21, 169–189.

Kemp, A.E.S., Pearce, R.B., Koizumi, I., Pike, J., Rance, S.J., 1999. The role of mat-forming diatoms in the formation of Mediterranean sapropels. Nature 398, 57–61.

Kidd, R.B., Cita, M.B., Ryan, W.B.F., 1978. Stratigraphy of eastern Mediterranean sapropel sequences recovered during DSDP Leg 42A and their paleoenvironmental significance. Init. Rep. Deep Sea Drilling Proj. 42A, 421–443.

Klein, B., Roether, W., Manca, B.B., Bregant, D., Beitzel, V., Kovacevic, V., Luchetta, A., 1999. The large deep water transient in the Eastern Mediterranean. Deep-Sea Research I 46, 371–414.

Langereis, C.G., Dekkers, M.J., De Lange, G.J., Paterne, M., Van Santvoort, P.J.M., 1997. Magnetostratigraphy and astronomical calibration of the last 1.1 Myr from a Central Mediterranean piston core and dating of short events in the Brunhes. Geophys. J. Int. 129, 75–94.

Leaman, K.D., Schott, F.A., 1991. Hydrographic structure of the convection regime in the Gulf of Lions: Winter, 1987. Journal of Physical Oceanography 21, 575–598.

Leventhal, J.S., 1995. Carbon-sulfur plots to show diagenetic and epigenetic sulfidation in sediments. Geochim. Cosmochim. Acta 59, 1207–1211.

Lourens, L.J., Antonarakou, A., Hilgen, F.J., Van Hoof, A.A.M., Vergnaud-Grazzini, C., Zachariasse, W.J., 1996. Evaluation of the Plio-Pleistocene astronomical timescale. Paleoceanography 11, 391–413.

Lyons, T.W., Berner, R.A., 1992. Carbon-sulfur-iron systematics of the uppermost deep-water sediments of the Black Sea. Chem. Geol. 99, 1–27.

Mariolopoulos, E.G. 1961. An outline of the climate of Greece, Publications of the Meteorological Institute of the University of Athens 6, 51 pp.

McManus, J., Berelson, W.M., Klinkhammer, G.P., Kilgore, T.E., Hammond, D.E., 1994. Remobilisation of barium in continental margin sediments. Geochim. Cosmochim. Acta 58, 4899–4908.

McManus, J., Berelson, W.M., Klinkhammer, G.P., Johnson, K.S.,

Coale, K.H., Anderson, R.F., Kumar, N., Burdige, D.J., Hammond, D.E., Brumsack, H.J., McCorkle, D.C., Rushdi, A., 1998. Geochemistry of barium in marine sediments; implications for its use as a paleoproxy. Geochim. Cosmochim. Acta 62, 3453–3473.

Malanotte-Rizzoli, P., Hecht, A., 1988. Large-scale properties of the Eastern Mediterranean: a review. Oceanologica Acta 11, 323–335.

Mercone, D., Thomson, J., Croudace, I.W., Siani, G., Paterne, M., Troelstra, S., 2000. Duration of S1, the most recent Mediterranean sapropel, as indicated by AMS radiocarbon and geochemical evidence. Paleoceanography 15, 336–347.

Myers, P.G., Haines, K., Rohling, E.J., 1998. Modeling the paleocirculation of the Mediterranean: The last glacial maximum and the Holocene with emphasis on the formation of sapropel S1. Paleoceanogr. 13, 586–606.

Nijenhuis, I.A., Bosch, H.J., Sinninghe Damste, J.S., Brumsack, H.-J., De Lange, G.J., 1999. Organic matter and trace element rich sapropels and black shales; a geochemical comparison. Earth. Planet. Sci. Lett. 169, 277–290.

Passier, H.F., Middelburg, J.J., van Os, B.J.H., de Lange, G.J., 1996. Diagenetic pyritisation under eastern Mediterranean sapropels caused by downward sulphide diffusion. Geochim. Cosmochim. Acta 60, 751–763.

Passier, H.F., de Lange, G.J., 1998. Sediemntary sulphur and iron chemistry in relation to the formation of eastern Mediterranean sapropels. Proceedings of the Ocean Drilling Program: Scientific Results 160, 249–259.

Passier, H.F., Middelburg, J.J., de Lange, G.J., Bottcher, M.E., 1999. Modes of sapropel formation in the eastern Mediterranean: some constraints based on pyrite properties. Mar. Geol. 153, 199–219.

Piper, D.Z., 1994. Seawater as the source of minor elements in black shales, phosphorites and other sedimentary rocks. Chemical Geology 114, 95–114.

Poulos, S.E., Drakopoulos, P.G., Collins, M.B., 1997. Seasonal variability in sea surface oceanographic conditions in the Aegean Sea (eastern Mediterranean): an overview. J. Mar. Sys. 13, 225–244.

Price, N.B., Calvert, S.E., 1977. The contrasting geochemical behaviours of iodine and bromine in sediments from the Namibian Shelf. Geochim. Cosmochim. Acta 41, 1769–1775.

Raiswell, R., Berner, R.A., 1986. Pyrite and organic matter in Phanerozoic normal marine shales. Geochim. Cosmochim. Acta 50, 1967–1976.

Raiswell, R., Buckley, F., Berner, R.A., Anderson, T.F., 1988. Degree of pyritization of iron as a paleoenvironmental indicator of bottom-water oxygenation. J. Sediment. Petrol. 58, 812–819.

Rohling, E.J., 1994. Review and new aspects concerning the formation of eastern Mediterranean sapropels. Mar. Geol. 122, 1–28.

Rohling, E.J., Gieskes, W.W.C., 1989. Late Quaternary changes in Mediterranean Intermediate Water density and formation rate. Paleoceanography 4, 531–545.

Rohling, E.J., Hilgen, F.J., 1991. The eastern Mediterranean climate at times of sapropel formation: a review. Geol. Mijnbouw 70, 253–264.

Rohling, E.J., Jorissen, F.J., De Stigter, H.C., 1997. 200 year interruption of sapropel formation in the Adriatic Sea. J. Micropalaeontol. 16, 97–108.

Rossignol-Strick, M., 1983. African monsoons, an immediate climate reponse to orbital insolation. Nature 304, 46–49.

Rossignol-Strick, M., 1985. Mediterranean Quaternary sapropels, an immediate response of the African monsoon to variations in insolation. Palaeogeogr. Palaeoclimatol. Palaeoecol. 49, 237–263.

Rossignol-Strick, M., Nesteroff, W., Olive, P., Vergnaud-Grazzini, C., 1982. After the deluge: Mediterranean stagnation and sapropel formation. Nature 295, 105–110.

Ryan, W.F.B., 1972. Stratigraphy of Late Quaternary sediments in the eastern Mediterranean. In: Stanley, D.J. (Ed.), The Mediterranean Sea. Dowden, Hutchinson and Ross, Stroudsbury, PA, pp. 149–160.

Shaw, T.J., Gieskes, J.M., Jahnke, R.A., 1990. Early diagenesis in differing depositional environments: The response of transition metals in pore water. Geochim. Cosmochim. Acta 54, 1233–1246.

Schrader, H.J., Matherne, A., 1981. Sapropel formation in the eastern Mediterranean Sea: evidence from preserved opal assemblages. Micropaleontology 27, 191–203.

Shimmield, G.B., Pedersen, T.F., 1990. The geochemistry of reactive trace metals and halogens in hemipelagic continental margin sediments. Rev. Aquatic Sci. 3, 255–279.

Ten Haven, H.L., De Leeuw, J.W., Schenk, P.A., Klaver, G.T., 1987. Geochemistry of Mediterranean sediments. Bromine/organic carbon and uranium/organic carbon ratios as indicators for different sources of input and post-depositional oxidation, respectively. Org. Geochem. 13, 255–261.

Theocharis, A., Nittis, K., Kontoyiannis, H., Papageorgiou, E., Balapoulos, E., 1999. Climatic changes in the Aegean Sea influence the Eastern Mediterranean thermohaline circulation (1986–1997). Geophys. Res. Lett. 26, 1617–1620.

Thomson, J., Higgs, N.C., Wilson, T.R.S., Croudace, I.W., de Lange, G.J., van Santvoort, P.J.M., 1995. Redistribution and geochemical behaviour of redox-sensitive elements around S1, the most recent Eastern Mediterranean sapropel. Geochim. Cosmochim. Acta 59, 3487–3501.

Thomson, J., Mercone, D., de Lange, G.J., van Santvoort, P.J.M., 1999. Review of recent advances in the interpretation of Eastern Mediterranean sapropel S1 from geochemical evidence. Mar. Geol. 153, 77–89.

Turekian, K.K., Wedepohl, K.H., 1961. Distribution of the elements in some major units of the Earth's crust. GSA Bulletin 72, 175–192.

Van Os, B.J.H., Middelburg, J.J., de Lange, G.J., 1991. Possible diagenetic remobilisation of barium in sapropelic sediment from the eastern Mediterranean. Mar. Geol. 100, 125–136.

Van Os, B.J.H., Lourens, L.J., Hilgen, F.J., De Lange, G.J., Beaufort, L., 1994. The formation of Pliocene sapropels and carbonate cycles in the Mediterranean: diagenesis, dilution and productivity. Paleoceanography 9, 601–617.

van Santvoort, P.J.M., de Lange, G.J., Thomson, J., Cussen, H., Wilson, T.R.S., Krom, M.D., Strohle, K., 1996. Active post-depositional oxidation of the most recent sapropel (S1) in the

eastern Mediterranean. Geochim. Cosmochim. Acta 60, 4007–4024.

Vergnaud-Grazzini, C., Ryan, W.B.F., Cita, M.B., 1977. Stable isotope fractionation, climate change and episodic stagnation in the eastern Mediterranean during the late Quaternary. Mar. Micropaleontol. 2, 353–370.

Wanty, R.B., Goldhaber, M.B., 1992. Thermodynamics and kinetics of reactions involving vanadium in natural systems: Accumulation of vanadium in sedimentary rocks. Geochim. Cosmochim. Acta 56, 1471–1483.

Wehausen, R., Brumsack, H.-J., 1999. Cyclic variations in the chemical composition of eastern Mediterranean Pliocene sediments: a key for understanding sapropel formation. Mar. Geol. 153, 161–176.

Wignall, P.B., 1994. Black Shales. Oxford Monographs on Geology and Geophysics, Vol. 30. University of Oxford Press, Oxford, p. 127.

Wilkin, R.T., Barnes, H.L., 1996. Pyrite formation by reactions of iron monosulfides with dissolved inorganic and organic sulfur species. Geochim. Cosmochim Acta 60, 4167–4179.